Original Article

Effect of intravitreal and intraperitoneal cyanidin-3-glucoside injection in oxygen-induced retinopathy mouse model

Zeynep E Ercan, Nihan Haberal[1], Fatma Helvacıoglu[2], Atilla Dağdeviren[2], Gürsel Yılmaz

Purpose: To evaluate the effect of cyanidin-3-glucoside (C3G) in oxygen-induced retinopathy (OIR) mouse model. **Methods:** In this experimental study, 10 C57BL / 6J type mice exposed to room air comprised two control groups (n = 5 each; a negative control and a group receiving intravitreal sterile dimethyl sulfoxide [IVS DMSO]). Thirty C57BL / 6J type mice exposed to 75% ± 2% oxygen from postnatal day 7 to postnatal day 12 comprised the OIR groups. On postnatal day 12, these mice were randomized into six groups (n = 5 each): two OIR control groups (negative control and IVS DMSO), two intravitreal C3G groups (300 and 600 ng/μL), and two intraperitoneal C3G groups (0.05 and 0.1 mg/kg). We quantified neovascularization by counting endothelial cell proliferation on the vitreal side of the inner limiting membrane of the retina and examined histological and ultrastructural changes via light and electron microscopy and apoptosis by terminal deoxynucleotidyl transferase deoxy-UTP-nick end labeling. **Results:** The intravitreal C3G groups yielded lower endothelial cell counts compared with the intravitreal DMSO group. The intraperitoneal high-dose group had lower cell counts compared with the OIR control groups. Electron microscopy revealed significantly less mitochondrial dysmorphology in intravitreal groups and the high-dose intraperitoneal mice. We noted no difference in apoptotic cell count between the controls, low-dose intravitreal, and both intraperitoneal groups. However, apoptotic cell count was significantly higher in the high-dose intravitreal group. **Conclusion:** C3G suppresses endothelial cell proliferation in an OIR mouse model, leads to a reduced hyperoxia-induced mitochondrial dysmorphology, but increases apoptotic cell death in high concentrations.

Access this article online

Website: www.ijo.in

DOI: 10.4103/ijo.IJO_166_18

Quick Response Code:

Key words: Anthocyanin, cyanidin-3-glucoside, oxygen-induced retinopathy mouse model, retinal vascular disease, retinopathy of prematurity

Pathological retinal angiogenesis is a final common pathway leading to vision loss in neovascular ocular diseases, such as retinopathy of prematurity (ROP), diabetic retinopathy, and age-related macular degeneration.[1] ROP is characterized by two critical phases: hyperoxia and inflammation-induced damage to retinal vessels followed by hypoxia-driven physiological revascularization and pathologic neovascularization. The processes are largely driven by the hypoxia-induced factor-1α signaling pathway and vascular endothelial growth factor (VEGF) levels in the retina.[2] The retina is considered to be vulnerable to oxidative damage due to the abundance of polyunsaturated fatty acids, a high metabolic rate, and the rapid rate of oxygen consumption of the photoreceptors, and a reduced ability to scavenge reactive oxidative species (as seen in premature infants).[3] The increased levels of hypoxia-inducible and proinflammatory factors, such as Cyclooxygenase, Nitric oxide synthase, Platelet activating factor, Thromboxane A2 and Tumor necrosis factor-α, also contributes to ROP pathogenesis.[4,5]

Anthocyanins are common components of fruits and vegetables; in edible berries, anthocyanins provide pigmentation and show antioxidant, antiinflammatory, and anticarcinogenic effects.[6,7] In addition, the intravitreal administration of bilberry extract containing multiple anthocyanins was shown to inhibit the formation of neovascular tufts in oxygen-induced retinopathy (OIR) of mice.[8] Among these, cyanidin-3-glucoside (C3G)—the main anthocyanin in the edible parts of several plants—has been found to have the highest oxygen radical absorbance capacity.[9] It was shown to have inhibitory effects on proinflammatory cytokines and oxidative stress pathways that are active in the formation of senile macular degeneration.[10]

The aim of our study was to investigate the effects of intravitreal and intraperitoneal C3G at different concentrations on retinal endothelial cell proliferation, apoptotic cell death, and retinal morphology *in vivo* in the OIR mouse model.

Methods

Procedures for this study were in line with the Association for Research in Vision and Ophthalmology's Statement

Departments of Ophthalmology, [1]Pathology, [2]Histology and Embryology, Baskent University, Ankara, Turkey

Correspondence to: Dr. Zeynep Eylül Ercan, Turhal State Hospital, Ophthalmology Clinic, 60300, Turhal, Tokat, Turkey. E-mail: dreylulercan@gmail.com

Manuscript received: 01.02.18; Revision accepted: 05.07.18

Cite this article as: Ercan ZE, Haberal N, Helvacıoglu F, Dağdeviren A, Yılmaz G. Effect of intravitreal and intraperitoneal cyanidin-3-glucoside injection in oxygen-induced retinopathy mouse model. Indian J Ophthalmol 2019;67:801-5.

for the Use of Animals in Ophthalmic and Vision Research and were approved by the local animal care committee. One-way ANOVA performed with SPSS Statistics 24.0 (SPSS Inc., Chicago, IL, USA) was used to determine the significance between the groups. *P* values < 0.05 were considered statistically significant. *Post hoc* tests were used to identify differences among the groups.

The ROP model explained by Smith *et al.* was used in this study.[11] Ten newborn C57BL/6J type mice exposed to room air (21% oxygen) comprised the two control groups; fivemice in Group A served as negative control, and five mice in group B-S received 1 μL intravitreal sterile dimethyl sulfoxide (DMSO). Thirty newborn C57BL/6J type mice comprising the OIR group were exposed to 75% ± 2% oxygen from postnatal day 7 to postnatal day 12 with their nursing mothers. On the twelfth postnatal day, the OIR mice were returned to room air and randomized into six test groups of five mice each. C3G (purity, ≥98.80%; Biopurify Phytochemicals) was dissolved in sterile DMSO (Sigma-Aldrich) and stored at −40°C. This solution was diluted with DMSO to get 300 and 600 ng/μL for intravitreal use administered via a 32-gauge needle and a Hamilton syringe into the right eye. The mice were deeply anesthetized via intraperitoneal injection of ketamine hydrochloride (40 mg/kg) and xylazine hydrochloride (5 mg/mL). Group C served as the OIR control (receiving no injection). Group D-S was the injection control group receiving 1 μL intravitreal sterile DMSO. Group E received 300 ng/μL intravitreal C3G (IVC; the low-dose IVC group), and Group F received 600 ng/μL IVC (the high-dose IVC group). Group G received 0.05 mg/kg intraperitoneal C3G (IPC; the low-dose IPC group), and Group H received 0.1 mg/kg IPC (the high-dose IPC group).

All injections were administered on postnatal day 12, and, on postnatal day 17, the mice were humanely killed before enucleation with the intraperitoneal injection of ketamine hydrochloride (100 mg/kg) and xylazine hydrochloride (5 mg/mL). Enucleated eyes were examined via light microscopy (LM) and electron microscopy (EM). The extent of apoptosis was investigated using the terminal deoxynucleotidyl transferase-mediated nick end labeling (TUNEL) technique using the same paraffin sections used for LM.

LM

Enucleated eyes were fixed with 4% formalin and embedded in paraffin for LM evaluation. Serial sections of the retina (4-μm thick) were obtained starting at the optic disc. The second or third sections after the optic disc were taken for evaluation. One section per eye was evaluated. For the quantitative assessment of retinal neovascularization, periodic acid-Schiff and hematoxylin stained serial sections were used. We quantified neovascularization by counting the endothelial cell proliferation on the vitreal side of the inner limiting membrane for each histological section of the retina. In the morphological analysis of the retinal layers, we investigated any findings of cystic degeneration, hypocellularity, or loss of the nuclear layer in each group. Slides were examined using LM (OLYMPUS BX51, Germany). For the quantitative assessment of retinal neovascularization, endothelial cell nuclei counts are shown as the mean ± standard deviation.

EM

Tissue fixation was made using a phosphate buffer containing 2.5% glutaraldehyde and then fixed in 1% osmium tetroxide followed by dehydration in graded alcohols. They were embedded in Araldyte® CY 212, 2-dodecenyl succinic anhydride, benzyldimethyl amine, and dibutyl phthalate after passing through propylene oxide. 1% Toluidine Blue were used to stain the semithin sections. Ultrathin sections stained with uranyl acetate and lead citrate were examined with an LEO 906E EM transmission electron microscope.

We evaluated the ultrastructural morphology of the inner and outer photoreceptor layers in each group using EM. Two independent observers performed the EM and LM assessment of masked retinal tissue samples.

TUNEL technique

Four micrometer (4 μm) thick serial sections starting from the optic disc were obtained, and stained with hematoxylin–eosin. One section per eye was evaluated. Two independent observers used LM (OLYMPUS BX51) to look for TUNEL-positive cells in masked. Apoptotic TUNEL-positive cells were measured in 10 randomly selected fields on each slide.

Results

The OIR groups and the results are shown in Fig. 1. Hyperoxia-induced neovascularization was measured by counting the endothelial cell nuclei on the vitreal side of the ILM. There was no statistically significant change between Group A and Group B-S (*P* = 0.88). In Group C, the retina contained multiple neovascular tufts extending into the vitreous, originating from retinal vessels and forming clusters of immature endothelial cells [Fig. 2]. The results are Group D-S revealed no statistically significant change compared with Group C (*P* = 0.165). As for the IVC groups, endothelial cell nuclei counts were 6.3 ± 1.3 for Group E (low-dose IVC) and 5.6 ± 1.3 for Group F (high-dose IVC), but the difference between them was not statistically significant (*P* = 0.57). On the other hand, compared with Group D-S, both had significantly fewer endothelial cell nuclei (*P* < 0.0001 each). The Group G (low-dose IPC) cell count was similar to the nontreatment OIR control Group C (*P* = 0.098). In contrast, Group H (high-dose IPC) had a significantly lower cell count of 15.3 ± 1.3 compared with Group C (p < 0.0001). However, its effect on neovascularization was not as significant as the effect seen in the IVC groups (p < 0.0001).

Ultrastructural analysis with EM

Atypical mitochondria with mottled matrix and electron-dense bodies in the central region of cristae surrounded by lytic matrix and extensive cristalysis were used to quantify the mitochondrial dysmorphology in the groups. We counted the numbers of these in the fields of view using the same magnification (×6000) for each sample in a given area in each group [Fig. 3]. There was no significant difference between the IVC groups; both showed a decrease in atypical mitochondria counts compared with Group D-S (p < 0.0001). There was no significant difference between the low-dose IPC Group G and control Group C (*P* = 0.61), but a significantly lower count was noted in the high-dose IPC Group H compared with Groups C and D-S (*P* < 0.0001 each). Atypical mitochondria counts were similar in the IVC groups and Group H with no statistically significant difference (*P* = 0.89).

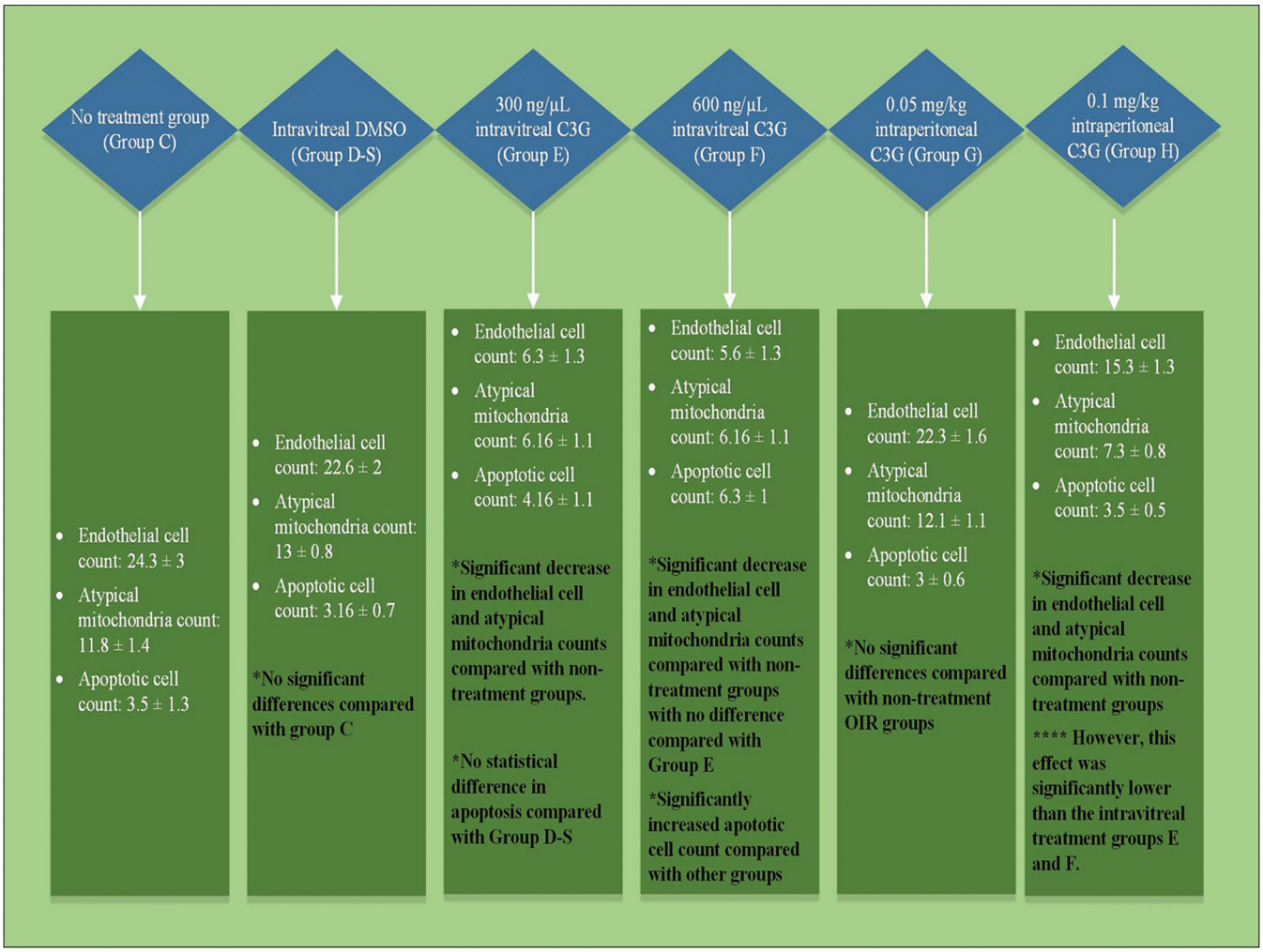

Figure 1: OIR group results

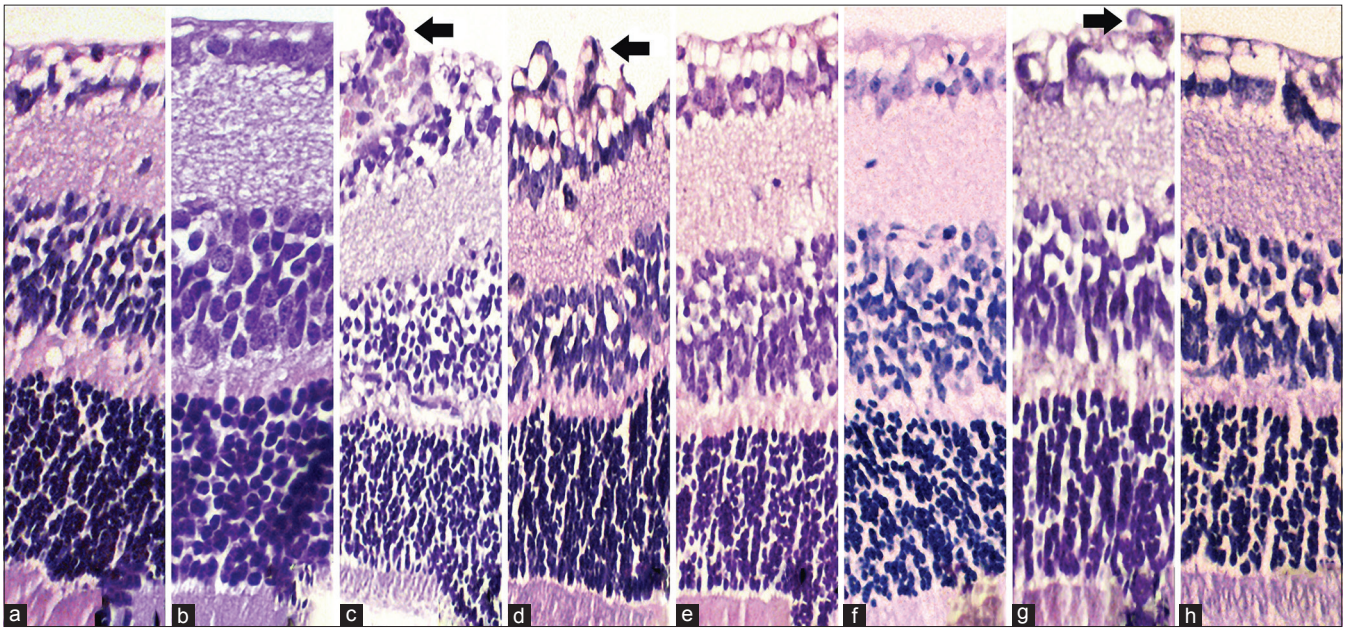

Figure: 2: Light micrographs of C57BL/6J mouse retina. Serial sections of the retina (4 µm thick), starting from the optic disc with the second sections after the optic disc taken for evaluation. The arrows in slides c, d, and g indicate endothelial cell proliferation, which are respectively the OIR nontreatment group, OIR DMSO-injected group and the low dose IPC group. Slides a and b have no proliferation, whereas slides e,f and h have significantly less compared with c,d and g. Original magnification ×20

Apoptosis analysis with TUNEL technique

We determined the number of TUNEL-positive cells in each sample, and found no statistically significant difference (P = 0.74) between Group D-S and the IVC Group E. No statistically significant difference was noted between IPC Groups G and H (P = 0.74). IPC groups were also statistically no different than Group C (P = 0.99 each) or low-dose IVC group (P = 0.57 and P = 0.79, respectively). The number of TUNEL-positive cells in high-dose IVC group was statistically significantly greater compared with other groups (Group D P < 0.0001, Group E P = 0.025, Group G P < 0.0001 and Group H P = 0.012) [Fig. 4].

Discussion

In this study, we report, for the first time, the effect of a single anthocyanin type (C3G) in different concentrations in OIR of mice. We have found that 300 and 600 ng/μL intravitreal C3G are both effective in reducing neovascularization and atypical mitochondria. A total of 0.1 mg/kg intraperitoneal C3G was also shown to have similar, albeit diminished effect. However, apoptosis was also increased in 600 ng/μL intravitreal C3G group.

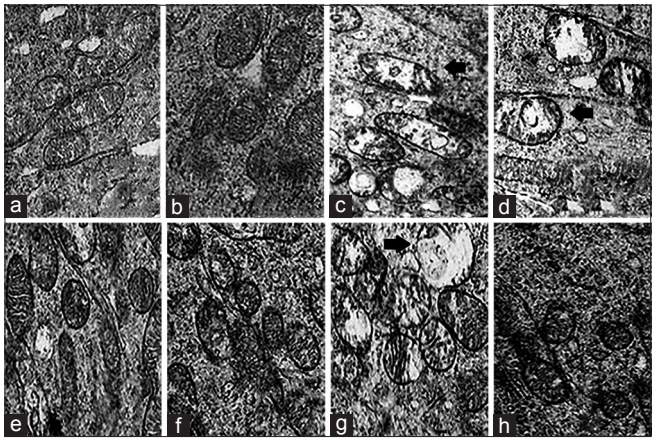

Figure 3: Electron micrograph showing mitochondrial morphology. Arrows in slides c, d, and g indicate atypical mitochondria with mottled matrix and electron-dense bodies in the cristae central region surrounded by lytic matrix and extensive cristalysis. Note their increase in slide g (low dose IPC group). Slide a and b have none, whereas slides e,f and h have significantly less compared with c,d and g

Anthocyanins, which can be used in various ways for their antioxidant, antiinflammatory, and neuroprotective effects, are the main protective compound in different berry types.[12,13] The fluctuating oxygen tensions in premature retinopathy result in retinal hypoxia, triggering the overproduction of reactive oxygen species (ROS) and inducing oxidative stress damage in preterm infants who have a natural inadequacy of antioxidant levels.[14] This overproduction of ROS activates NADPH oxidase and the JAK/STAT pathway, contributing to intravitreal neovascularization formation.[15] Inhibiting Nuclear factor-kappa beta activation was also shown to reduce retinopathy in ROP animal models—a pathway that can be suppressed by anthocyanins.[16] Matsunaga *et al.* showed that bilberry extracts containing anthocyanins inhibit endothelial cell proliferation, migration, and phosphorylations of Extracellular signal-regulated kinases 1/2 and Akt (Protein kinase B), induced by VEGF-A *in vitro* and decreased neovascular tuft formation in the *in vivo* OIR model.[17,18] In this study, we found a decrease in retinal endothelial cell count with different concentrations of IVC. Both high and low doses of C3G were effective in suppressing neovascularization without significant statistical difference between the doses. When injected intraperitoneally, 0.05 mg/kg C3G demonstrated no effect on the OIR model. Doubling C3G concentration to 0.1 mg/kg efficiently inhibited neovascularization, albeit to a significantly lesser extent than the IVC groups. The atypical mitochondria count by EM showed a similar result, mainly, a decrease in mitochondrial damage in both IVC groups and the 0.1 mg/kg IPC group. This effect on mitochondrial damage is also consistent with the results presented in the literature. Song *et al.* demonstrated that blueberry anthocyanins can increase the total antioxidant capacity of the retina.[19] Perveen *et al.* suggested that C3G inhibits ATP-induced calcium signaling in a protein kinase-independent manner and blocks ATP-induced formation of ROS and mitochondrial depolarization.[20]

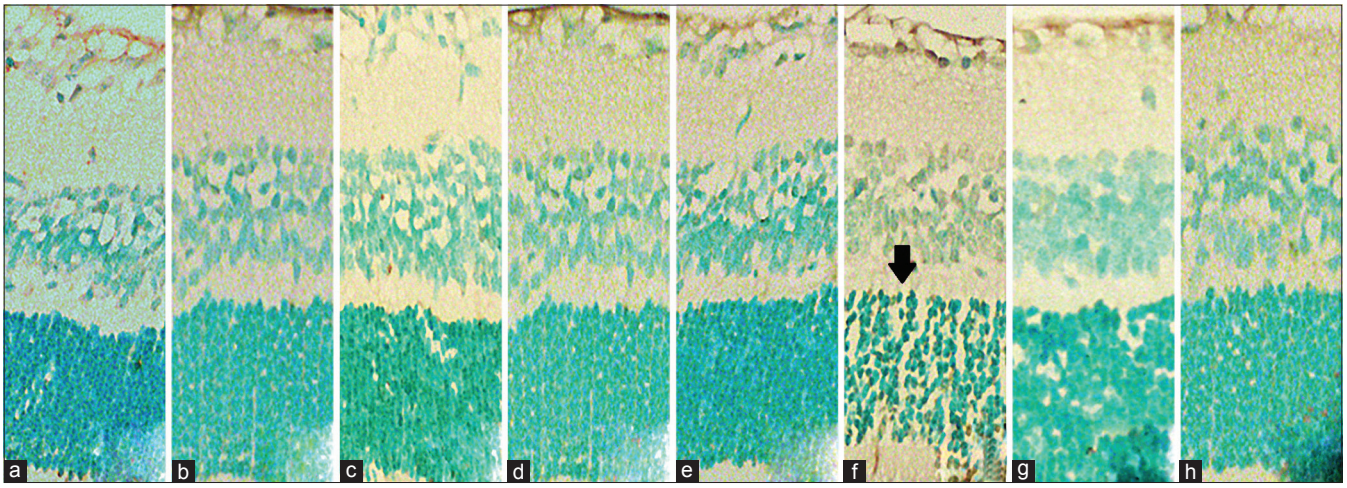

Figure 4: Light micrographs showing assessed apoptotic cells using the TUNEL assay. Apoptotic cells appear distinct deep pigmented (arrow) in the outer nuclear layer and inner nuclear layer in each group. Note the high amount of apoptosis in slide f, the 600-ng/μL IVC group. Apoptotic cell counts of slides a,b,c,d,e,g and h have no statistical difference within each other. Original magnification ×100, oil immersion

In this study, apoptosis increased in the high-dose IVC group. This result was not unexpected considering the mix apoptotic effects of C3G shown in the literature. The C3G effect of caspase-3 inhibition, which helps prevent apoptosis, was documented by Anwar *et al*. in C3G pretreated endothelial cells exposed to hypoxic conditions.[21] Skemiene *et al*. also showed that pretreatment with anthocyanins can block ischemia and caspase activation in cardiac cells.[22] However, in other studies, C3G is reported as proapoptotic, activating caspase pathway in malignant cells.[23] In N-methyl-D-aspartic acid-induced retinal damage, intravitreous co-injection of anthocyanins significantly reduced the morphological retinal damage and the amount of TUNEL-positive cells in the ganglion cell layer.[17] These results could be due to the cellular structure and pH changes. Radical scavenging activities of C3G are dependent on pH changes, so hyperoxia and ischemia induced intracellular acidosis might be interfering with C3G activity. In this case, starting C3G treatment within the same time of high-dose oxygen inducement may give different results.[24,25] And since 300 ng IVC has same effectivity with 600 ng IVC in lowering the endothelial cell and atypical mitochondria count, 600 ng IVC could be a far more concentrated intravitreal dose than needed for the treatment of OIR.

Conclusion

In conclusion, we believe C3G can be used in a dose-dependent manner as an adjunct therapy for OIR. However, further studies are needed to evaluate its cell toxicity dose, mechanism and efficacy changes with acidosis and interactions with anti-VEGF treatments.

Financial support and sponsorship

Nil.

Conflicts of interest

There are no conflicts of interest.

References

1. Asano MK, Dray PB. Retinopathy of prematurity. Dis Mon 2014;60:282-291.
2. Cavallaro G, Filippi L, Bagnoli P, La Marca G, Cristofori G, RaffaeliG, *et al*. The pathophysiology of retinopathy of prematurity: An update of previous and recent knowledge. Acta Ophthalmol 2014;92:2-20.
3. Saito Y, Geisen P, Uppal A, Hartnett ME. Inhibition of NAD (P) H oxidase reduces apoptosis and avascular retina in an animal model of retinopathy of prematurity. Mol Vis 2007; 13:840-53.
4. Beauchamp MH, Marrache AM, Hou X, Gobeil F Jr, Bernier SG, Lachapelle P, *et al*. Platelet-activating factor in vasoobliteration of oxygen-induced retinopathy. Invest Ophthalmol Vis Sci 2002;43:3327-37.
5. Vadlapatla RK, Vadlapudi AD, Mitra AK. Hypoxia-inducible factor-1 (HIF-1): A potential target for intervention in ocular neovascular diseases. Curr Drug Targets 2013;14:919-35.
6. Seeram NP, Momin RA, Nair MG, Bourquin LD. Cyclooxygenase inhibitory and antioxidant cyanidin glycosides in cherries and berries. Phytomedicine 2001;8:362-9.
7. Acquaviva R, Russo A, Galvano F, Galvano G, Barcellona ML, Li Volti G, *et al*. Cyanidin and cyanidin 3-O-beta-D-glucoside as DNA cleavage protectors and antioxidants. Cell Biol Toxicol 2003;19:243-52.
8. Matsunaga N, Chikaraishi Y, Shimazawa M, Yokota S, Hara H. Vaccinium myrtillus (Bilberry) Extracts Reduce Angiogenesis *In Vitro* and *In Vivo*. Evid Based Complement Alternat Med 2010;7:47-56.
9. Dugo P, Mondello L, Errante G, Zappia G, Dugo G. Identification of anthocyanins in berries by narrow-bore high-performance liquid chromatography with electrospray ionization detection J Agric Food Chem 2001;49:3987-92.
10. Jin X, Wang C, Wu W, Liu T, Ji B, Zhou F. Cyanidin-3-glucoside Alleviates 4-Hydroxyhexenal-Induced NLRP3 Inflammasome Activation via JNK-c-Jun/AP-1 Pathway in Human Retinal Pigment Epithelial Cells. J Immunol Res 2018;2018:5604610.
11. Smith LE, Wesolowski E, McLellan A, Kostyk SK, D'Amato R, Sullivan R, *et al*. Oxygen-induced retinopathy in the mouse. Invest Ophthalmol Vis Sci 1994;35:101-11.
12. Bhuiyan MI, Kim HB, Kim SY, Cho KO. The Neuroprotective Potential of Cyanidin-3-glucoside Fraction Extracted from Mulberry Following Oxygen-glucose Deprivation. Korean J Physiol Pharmacol 2001;15:353-61.
13. Duymus HG, Goger F, Baser KH. *In vitro* antioxidant properties and anthocyanin compositions of elderberry extracts. Food Chem 2014;155:112-9.
14. Rivera JC, Sapieha P, Joyal JS, Duhamel F, Shao Z, Sitaras N, *et al*. Understanding retinopathy of prematurity: Update on pathogenesis. Neonatol 2011;100:343-53.
15. Byfield G, Budd S, Hartnett ME. The role of supplemental oxygen and JAK/STAT signaling in intravitreous neovascularization in a ROP rat model. Invest Ophthalmol Vis Sci 2009;50:3360-5.
16. Min HK, Kim SM, Baek SY, Woo JW, Park JS, Cho ML, *et al*. Anthocyanin Extracted from Black Soybean Seed Coats Prevents Autoimmune Arthritis by Suppressing the Development of Th17 Cells and Synthesis of Proinflammatory Cytokines by Such Cells, via Inhibition of NF-κB. PLoS One 2015;10:e0138201.
17. Matsunaga N, Imai S, Inokuchi Y, Shimazawa M, Yokota S, Araki Y, *et al*. Bilberry and its main constituents have neuroprotective effects against retinal neuronal damage *in vitro* and *in vivo*. Mol Nut Food Res 2009;53:869-77.
18. Matsunaga N, Tsuruma K, Shimazawa M, Yokota S, Hara H. Inhibitory actions of bilberry anthocyanidins on angiogenesis. Phytother Res. 2010;24(Suppl 1):S42-7.
19. Song Y, Huang L, Yu J. Effects of blueberry anthocyanins on retinal oxidative stress and inflammation in diabetes through Nrf2/HO-1 signaling. J Neuroimmunol 2016;301:1-6.
20. Perveen S, Yang JS, Ha TJ, Yoon SH. Cyanidin-3-glucoside Inhibits ATP-induced Intracellular Free Ca(2+) Concentration, ROS Formation and Mitochondrial Depolarization in PC12 Cells. Korean J Physiol Pharmacol 2014;18:297-305.
21. Anwar S, Speciale A, Fratantonio D, Cristani M, Saija A, Virgili F, *et al*. Cyanidin-3-O-glucoside modulates intracellular redox status and prevents HIF-1 stabilization in endothelial cells *in vitro* exposed to chronic hypoxia. Toxicol Lett 2014;226:206-213.
22. Skemiene K, Rakauskaite G, Trumbeckaite S, Liobikas J, Brown GC, Borutaite V. Anthocyanins block ischemia-induced apoptosis in the perfused heart and support mitochondrial respiration potentially by reducing cytosolic cytochrome c. Int J Biochem Cell Biol 2013;45:23-9.
23. Sorrenti V, Vanella L, Acquaviva R, Cardile V, Giofre S, Di Giacomo C. Cyanidin induces apoptosis and differentiation in prostate cancer cells. Int J Oncol 2015;47:1303-10.
24. Padnick-Silver L, Linsenmeier RA. Effect of hypoxemia and hyperglycemia on pH in the intact cat retina. Arch Ophthalmol 2005;123:1684-90.
25. Tirupula KC, Balem F, Yanamala N, Klein-Seetharaman J. pH-dependent interaction of rhodopsin with cyanidin-3-glucoside. 2. Functional aspects. Photochem Photobiol 2009;85:463-70.